Journal of Organometallic Chemistry, 479 (1994) 109–116

Easy triphenylphosphine replacement of a CO ligand in the dicarbene complex $[Fe_2(CO)_7\{\mu\text{-}C(R)C(NEt_2)\}]$. Syntheses and characterizations of $[Fe_2(CO)_6(PPh_3)\{\mu\text{-}C(R)C(NEt_2)\}]$

J.C. Daran, B. Heim, M. Gouygou and Y. Jeannin

Laboratoire de Chimie des Métaux de Transition, URA-CNRS 419, Université P. et M. Curie, 4 Place Jussieu, 75252 Paris cedex 05 (France)

(Received November 11, 1993)

Abstract

Triphenylphosphine reacts easily at room temperature with the dicarbene complex $[Fe_2(CO)_7\{\mu\text{-}C(R)C(NEt_2)\}]$ R = Me (**1a**); C_3H_5 (**1b**); $SiMe_3$ (**1c**); Ph (**1d**), to afford the monosubstituted complex $[Fe_2(CO)_6(PPh_3)\{\mu\text{-}C(R)C(NEt_2)\}]$ (**2**) (R = Me, C_3H_5, $SiMe_3$, Ph). All compounds were characterized by ^1H, ^{31}P and ^{13}C NMR and IR spectroscopies and chemical analysis. The molecular structures of **1d** and **2d** were determined by X-ray crystallography. Whatever the solvent used, only one isomer of any complex could be isolated. The incoming triphenylphosphine did not seem to influence the carbene structure.

Key words: Iron; Phosphorus; Dicarbene; Alkyne; X-ray diffraction; Nuclear magnetic resonance

1. Introduction

Recent studies in our laboratories have focussed on the reactivity of the dinuclear complex $[Fe_2(CO)_7\{\mu\text{-}C(R)C(NEt_2)\}]$ (**1**) (Scheme 1) which can be regarded as a dicarbene species [1].

Alkynes and heterocumulenes react with this complex through cycloaddition or insertion, involving either the terminal or the bridging carbene [2]. The first step in the attack of the incoming group was a puzzle. It is known that phosphine can be used to probe the chemical and structural properties of organometallic complexes [3], so it seemed worthwhile to investigate the effect of phosphine substitution on the reactivity of complex **1** in order to gain insight into the mechanism pathway.

This paper reports the syntheses and spectroscopic characterization of a series of complexes $[Fe_2(CO)_6(PPh_3)\{\mu\text{-}C(R)C(NEt_2)\}]$ (**2**) (R = Me, C_3H_5, $SiMe_3$, or Ph) resulting from the reaction of **1** with triphenylphosphine.

Correspondence to: Dr. J.C. Daran.

2. Results and discussion

2.1. Syntheses of complexes 1

The preparation of $[Fe_2(CO)_7\{\mu\text{-}C(R)C(NEt_2)\}]$ R = Me (**1a**), C_3H_5 (**1b**), $SiMe_3$ (**1c**), or Ph(**1d**) has been described elsewhere [1,2d,4]. For **1a**, **1b** and **1c**, the ynamine $RC \equiv CNEt_2$ reacted with $[Fe_2(CO)_9]$ in hexane at 0°C in the presence of Me_3NO to yield the aminocarbenediiron complexes **1**. However, subsequent studies [5] of the reactivity of **1** showed that the use of Me_3NO was not "innocent" and led to side reactions with slow decomposition of **1**. Synthesis of **1d** was then realized using a slightly different procedure. The *N,N*-diethyl(phenylethynyl)amine, $PhC \equiv CNEt_2$, was stirred overnight with $[Fe_2(CO)_9]$ in hexane (or dichloromethane) at room temperature without Me_3NO [4]. A similar procedure was carried out to synthesize the **1a**, **1b** and **1c** used in this study (Scheme 2).

All compounds were characterized by IR, ^1H NMR and mass spectroscopies. Crystal structures of **1a** [1] and **1c** [2(d)] have been reported previously so in order to compare structural features of all these complexes, the crystal structure of **1d** was determined by X-ray

0022-328X/94/$7.00
SSDI 0022-328X(93)24382-F

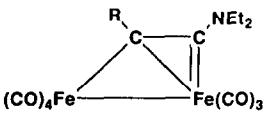

R= Me(1a), C_3H_5(1b), $SiMe_3$(1c), Ph(1d)

Scheme 1.

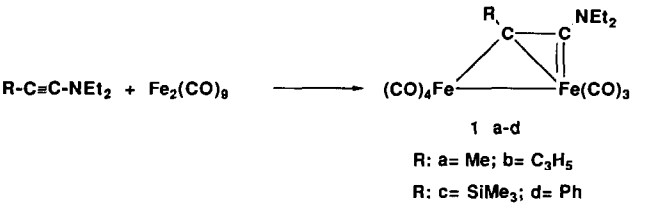

Scheme 2.

diffraction. A representation of the latter molecule is shown in Fig. 1.

As expected, the molecule was found to contain the *N*,*N*-diethyl(phenylethynyl)amine bridging two iron atoms asymmetrically. The C(1) atom is only bonded to Fe(2) with a short Fe–C bond distance, whereas the C(2) atom symmetrically bridges the two iron atoms. The observed bond distances within the "Fe_2C_2N" framework (Table 1) show that the geometry of the three complexes is identical within experimental error except for the metal–metal bond, which is slightly but significantly longer for **1d**. This lengthening may result from the steric influence of the phenyl group in the molecular packing. The planarity of the Fe(2), C(1), N(1) and C(2) atoms, with the largest deviation from the plane being 0.033 Å at C(1), and the short C(1)–N(1) and Fe(2)–C(1) bonds suggest electron delocalization along the N(1)-C(1)-Fe(2) chain for all these complexes.

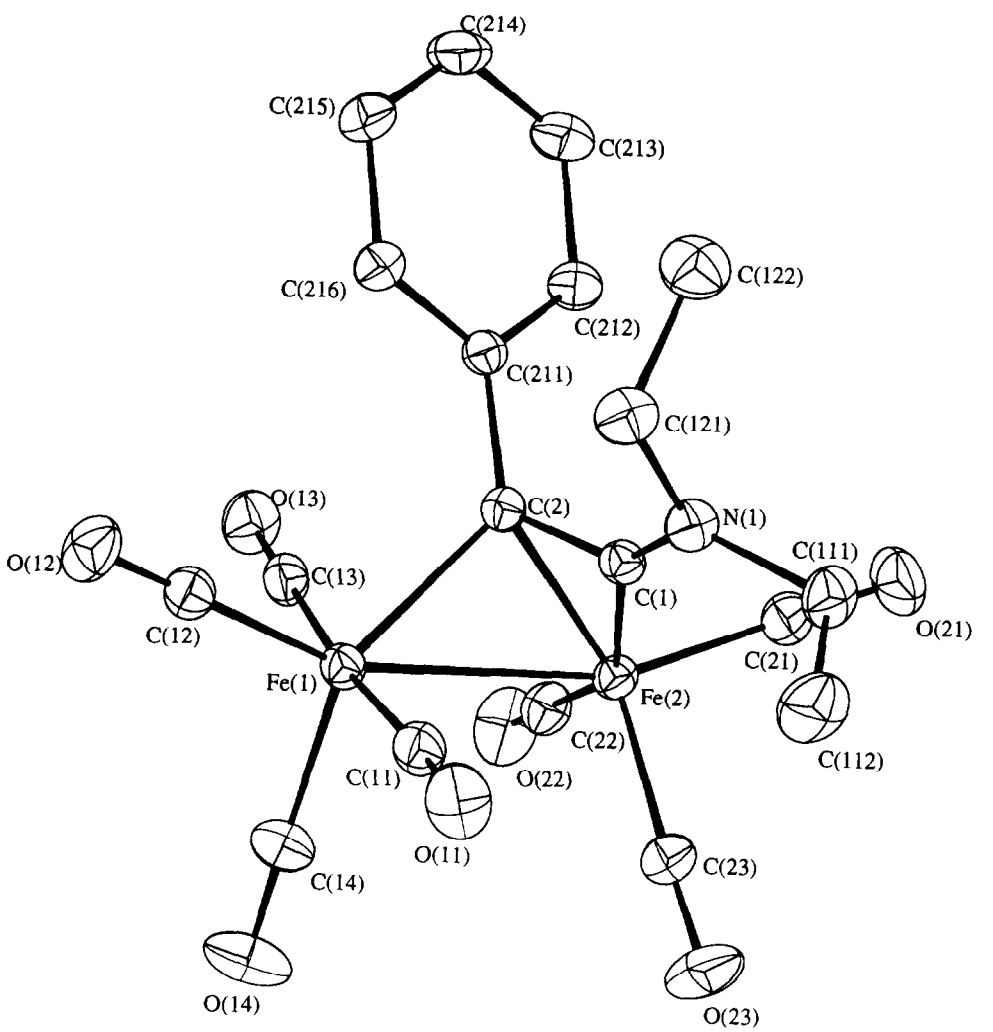

Fig. 1. Molecular structure of $[Fe_2(CO)_7\{C(Ph)C(NEt_2)\}]$ (**1d**) showing 30% probability thermal ellipsoids.

TABLE 1. Main interatomic distances (Å) within the "Fe_2C_2N" framework for complexes **1**

	R = Me(**1a**)	R = $SiMe_3$(**1c**)	R = Ph(**1d**)
Fe(1)–Fe(2)	2.617(3)	2.6181(5)	2.6333(6)
Fe(2)–C(1)	1.878(8)	1.883(2)	1.872(3)
Fe(2)–C(2)	2.007(9)	2.005(2)	2.016(3)
Fe(1)–C(2)	2.030(8)	2.068(2)	2.044(3)
C(1)–C(2)	1.369(9)	1.376(3)	1.391(4)
C(1)–N(1)	1.327(9)	1.300(3)	1.306(3)

Structurally, atom C(1) appears to possess significant carbene-like character. This is supported by the ^{13}C NMR spectrum of **1d**, which shows a low-field resonance for the C(1) carbon atom at 227 ppm. This deshielding may be compared with those observed for the carbene atom in aminocarbene complexes of chromium which exhibits a resonance at 267–270 ppm [6]. The partial multiple bonding between the alkynyl carbon C(1) and the nitrogen atom N(1) is reflected by the hindered rotation about this C–N bond in solution indicated by observation of separate resonances for the ethyl groups in the ^1H NMR spectra: two triplets for the inequivalent CH_3 groups and four multiplets related to the diasterotopic protons of the CH_2 groups. Similar observations have been reported by Adams *et al.* [7] for the related complexes $[Re_2(CO)_8\{C(Me)C(NMe_2)\}]$ and $[Mn_2(CO)_8\{C(Me)C(NMe_2)\}]$.

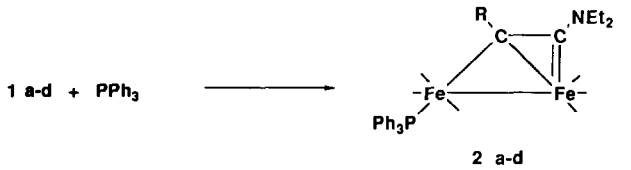

Scheme 3.

2.2. Syntheses of complexes 2 $[Fe_2(CO)_6(PPh_3)\{C(R)C(NEt_2)\}]$

^{31}P NMR spectroscopy (Table 2) shows that complex **1** undergoes quantitatively a mono-substitution reaction in the presence of PPh_3 whatever the solvent (hexane, dichloromethane, tetrahydrofuran) at room temperature to afford new complex **2** (Scheme 3).

Spectroscopic studies (^1H NMR, ^{31}P NMR, IR) (Table 2) and chemical analyses are in accordance with the formulation $[Fe_2(CO)_6(PPh_3)\{C(R)C(NEt_2)\}]$. The ^{31}P NMR resonance of complexes **2a–d** lies in the range 62.6–65 ppm. Good crystals of **2d** can be obtained by cooling a saturated hexane solution and the X-ray structure analysis was carried out to compare the

TABLE 2. IR and NMR Spectra of **1d** and **2a–d**

	IR (ν, cm^{-1})		NMR (at 25°C), δ	
1d	ν(CO)	2088s, 2026vs, 2012vs, 1997vs, 1981vs, 1957vs, 1941vs.	$^1H(C_6D_6)$	0.43 (t, 3H, N–CH_2–CH_3), 0.8 (t, 3H, N–CH_2–CH_3), 2.55 (m, 1H, N–CH_2–CH_3), 2.83 (m, 1H, N–CH_2–CH_3), 3.12 (m, 1H, N–CH_2–CH_3), 3.23 (m, 1H, N–CH_2–CH_3), 7.00 (m, 5H, C_6H_5)
	ν(C=N)	1617m	$^{13}C(C_6D_6)$	12.52 (s, C_{112} or C_{122}), 13.00 (s, C_{122} or C_{112}), 49.34 (s, C_{111} or C_{121}), 51.18 (s, C_{121} or C_{111}), 104.7 (s, C_2), 147.40 (s, C_{211}), 215 (s, C_{11-14} and C_{21-23}), 227 (s, C_1).
2a	ν(CO)	2025s, 1980vs, 1950vs, 1935vs, 1895sh.	$^1H(C_6D_6)$	0.79 (t, 3H, N–CH_2–CH_3), 0.91 (t, 3H, N–CH_2–CH_3), 2.46 (s, 3H, CH_3), 3.3 (m, 4H, N–CH_2–CH_3), 7.03 (m, 10H, $P(C_6H_5)_3$), 7.76 (m, 5H, $P(C_6H_5)_3$).
	ν(CN)	1630s	$^{31}P(C_6D_6)$	65.00 (s)
2b	ν(CO)	2040m, 1980s, 1950vs, 1930sh, 1913vs.	$^1H(C_6D_6)$	0.89 (m, 6H, N–CH_2–CH_3), 1.32 (m, 3H, CH_3–CH=CH), 3.05 (m, 1H, N–CH_2–CH_3), 3.14 (m, 1H, N–CH_3–CH_3), 3.33 (m, 1H, N–CH_2–CH_3), 3.56 (m, 1H, N–CH_2–CH_3), 4.92 (m, 1H, CH_3–CH=CH), 5.83 (m, 1H, CH_3–CH=CH), 7.74 (m, 15H, $P(C_6H_5)_3$)
	ν(CN)	1620m	$^{31}P(CDCl_3)$	62.60 (s)
2c	ν(CO)	2040m, 1980s, 1960vs, 1940vs, 1920vs,	$^1H(CDCl_3)$	0.26 (s, 9H, $Si(CH_3)_3$), 1.27 (t, 6H, N–CH_2–CH_3), 3.53 (q, *2H*, N–CH_2–CH_3), 3.78 (q, *2H*, N–CH_3–CH_3), 7.43 (m, 15H, $P(C_6H_5)_3$)
	ν(CN)	1610m	$^{31}P(CDCl_3)$	64.75 (s)
2d	ν(CO)	2031m, 1984vs, 1952vs, 1941vs.	$^1H(C_6D_6)$	0.68 (t, 3H, N–CH_2–CH_3), 0.91 (t, 3H, N–CH_2–CH_3), 2.88 (m, 1H, N–CH_2–CH_3), 3.2 (m, *2H*, N–CH_2–CH_3), 3.5 (m, 1H, N–CH_3–CH_3), 7.02 (m, 15H, $P(C_6H_5)_3$ and C_6H_5), 7.80 (m, 5H, $P(C_6H_5)_3$).
	ν(CN)	1616m	$^{31}P(C_6D_6)$	64.50 (s)
			$^{13}C(C_7D_8)$	14.37 (s, C_{112} or C_{122}), 14.78 (s, C_{122} or C_{112}), 51.46 (s, C_{111} or C_{121}), 51.68 (s, C_{121} or C_{111}), 100.60 (s, C_2), 136 (d, ^1J(C–P) = 45.5 H_z, C_{311}, C_{321} and C_{331}), 149.77 (s, C_{211}), 217.90 (s, C_{11-13} and C_{21-23}), 229.10 (s, C_1).

influence of coreplacement by phosphine on the geometry of the Fe_2C_2N framework.

The structure is very similar to that observed for **1d** (Fig. 2). The triphenylphosphine replaces a CO of the "$Fe(CO)_4$" group. The position of substitution is not *trans* to the Fe–Fe bond but *trans* to the bridging carbene atom C(2). This is, therefore, in direct contrast with observations reported for related complexes such as $[Fe_2(CO)_5PPh_3(C_8H_6S)]$ [8] and $[Fe_2(CO)_7PPh_3\{C(OEt)=CH(Me)\}]$ [9]. In the present case, the dominant factor influencing the position of substitution is steric, the incoming triphenylphosphine occupying the least hindered apex of the distorted octahedron surrounding Fe(1), remote from the bulky phenyl or diethylamino groups. A similar situation with the phosphine *cis* to the metal–metal bond and *trans* to a bridging phosphido-group was reported for $[Fe_2(CO)_5(PPh_3)(\mu\text{-}PPh_2)(C_2Ph)]$ [10]. The Fe(1)–P(3) bond distance for the title complex, 2.245(2) Å, is similar to the 2.235(2) distance in $[Fe_2(CO)_5PPh_3(C_8H_6S)]$ [8] or 2.2738(9) found in $[Fe_2(CO)_7PPh_3\{C(OEt)=CH(Me)\}]$ [9].

The Fe(1)–Fe(2) bond length, 2.645(1) Å, is slightly but significantly longer than for the unsubstituted complex **1d**, 2.6333(6) Å (Table 3). This small increase in the metal–metal bond distance is consistent with an increase in electron density on the substituted iron, but is also consistent with a steric argument, since the triphenylphosphine causes increased steric congestion about the metal as shown by the changes of the C–Fe(1)–C angles (Table 4). The C(2)–Fe(1)–X (X = C(14) or P(3)) angle increases dramatically from 147.8(1)° in **1d** to 166.7(2)° in **2d**, resulting in a nearly

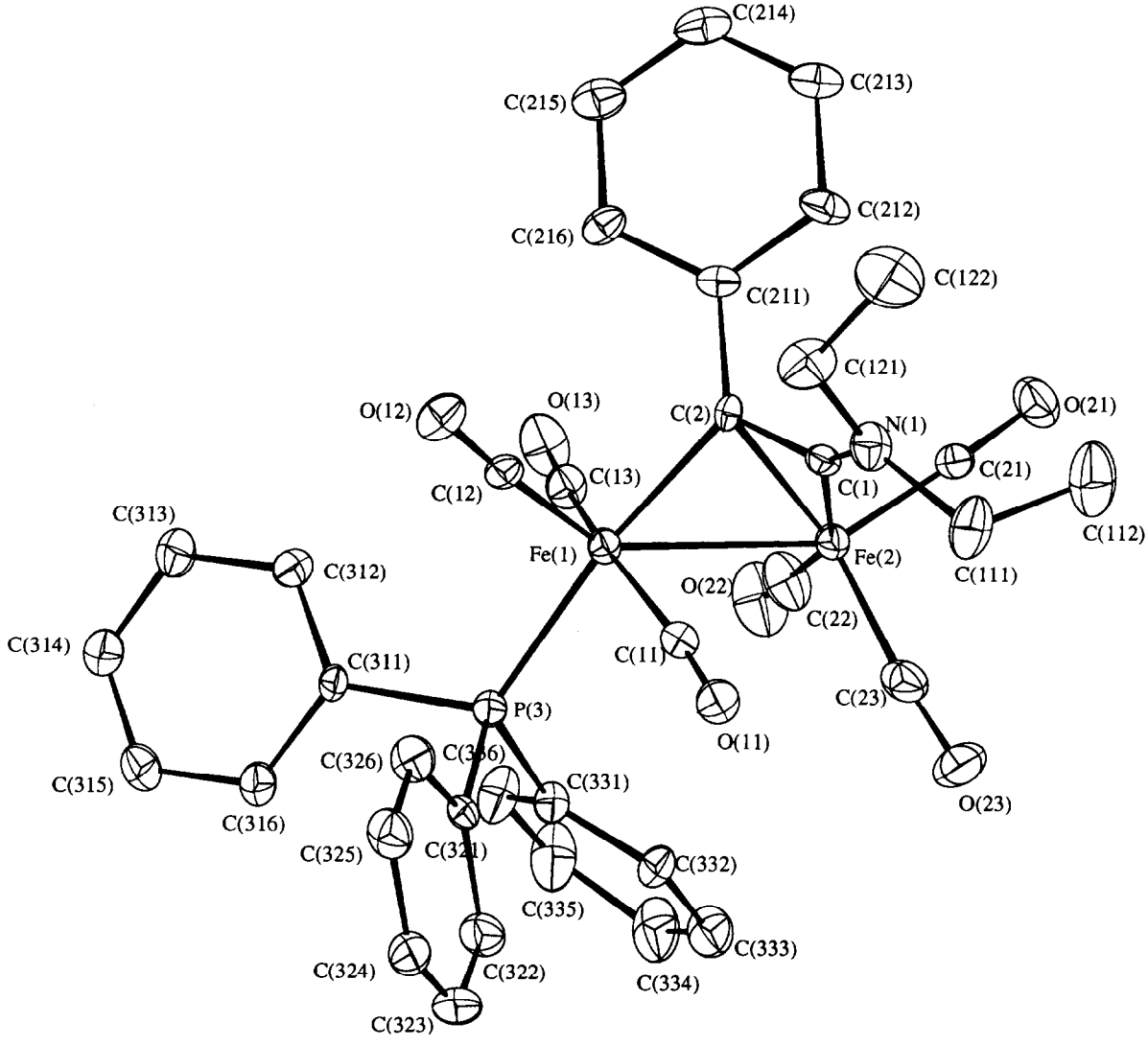

Fig. 2. Molecular structure of $[Fe_2(CO)_6(PPh_3)\{C(Ph)C(NEt_2)\}]$ (**2d**) showing 30% probability thermal ellipsoids.

TABLE 3. Selected interatomic distances (Å) for complexes **1d** and **2d**

	1d	2d
Fe(1)–Fe(2)	2.6333(6)	2.645(1)
Fe(2)–C(1)	1.872(3)	1.874(7)
Fe(2)–C(2)	2.016(3)	2.028(6)
Fe(1)–C(2)	2.044(3)	2.016(6)
C(1)–C(2)	1.391(4)	1.389(9)
C(1)–N(1)	1.306(3)	1.307(8)
Fe(1)–C(11)	1.816(3)	1.801(7)
Fe(1)–C(12)	1.790(3)	1.749(8)
Fe(1)–C(13)	1.818(3)	1.793(7)
Fe(1)–X	1.804(3)	2.245(2)
Fe(2)–C(21)	1.768(3)	1.738(8)
Fe(2)–C(22)	1.805(3)	1.803(9)
Fe(2)–C(23)	1.792(3)	1.771(9)

X = C(14) or P(3).

perfect *trans* siting of the phosphine with respect to the C(2) atom. The *trans* influence of the phosphine is reflected by a slightly but significantly shorter Fe(1)–C(2) distance in **2d**. Owing to the electron-withdrawing phenyl group, the excess of charge on the C(2) atom is released towards the ring, as reflected by the shorter C(2)–C(211) distance: 1.473(9) Å in **2d** instead of 1.492(4) Å in **1d**. Despite the above structural modifications, the Fe(1)–CO distances are identical within experimental error in both complexes. Moreover, except for the Fe(1)–C(2) distance, there are no significant differences between the "Fe_2C_2N" framework. The Fe–C, C–C and C–N distances do not appear to be influenced by the phosphine substitution (Table 3). The other bond distances and bond angles in the phenyl or diethylaminogroups do not deserve special comment and are in the ranges expected for these groups.

TABLE 4. Selected bond angles (°) for complexes **1d** and **2d**

	1d	2d
Fe(2)–C(1)–N(1)	148.7(2)	146.2(6)
C(2)–C(1)–N(1)	136.2(3)	138.5(7)
C(1)–N(1)–C(111)	121.2(3)	120.9(7)
C(1)–N(1)–C(121)	120.7(3)	120.1(6)
C(111)–N(1)–C(121)	118.0(2)	118.2(7)
Fe(2)–C(2)–Fe(1)	80.9(1)	81.7(2)
F(1)–C(2)–C(211)	126.4(2)	131.0(4)
Fe(2)–C(2)–C(211)	133.9(2)	131.6(5)
C(1)–C(2)–C(211)	123.3(2)	122.1(6)
C(2)–Fe(1)–C(11)	91.5(1)	94.7(3)
C(2)–Fe(1)–C(12)	107.8(1)	94.2(3)
C(2)–Fe(1)–C(13)	83.5(1)	85.1(3)
C(2)–Fe(1)–X	147.8(1)	166.7(2)
C(11)–Fe(1)–C(12)	92.1(1)	99.1(3)
C(11)–Fe(1)–C(13)	174.0(1)	158.2(4)
C(11)–Fe(1)–X	89.1(2)	87.0(2)
C(12)–Fe(1)–C(13)	92.5(1)	102.7(3)
C(12)–Fe(1)–X	104.3(2)	98.6(2)
C(13)–Fe(1)–X	93.3(1)	88.4(2)
C(1)–Fe(2)–C(21)	95.6(1)	95.7(3)
C(1)–Fe(2)–C(22)	150.0(1)	155.5(4)
C(1)–Fe(2)–C(23)	107.0(1)	104.8(4)
C(2)–Fe(2)–C(21)	111.6(1)	103.1(3)
C(2)–Fe(2)–C(22)	108.8(1)	114.0(4)
C(2)–Fe(2)–C(23)	137.0(1)	140.8(3)
C(21)–Fe(2)–C(22)	91.9(1)	91.7(4)
C(21)–Fe(2)–C(23)	97.6(1)	99.2(4)
C(22)–Fe(2)–C(23)	100.7(1)	97.0(5)

X = C(14) or P(3).

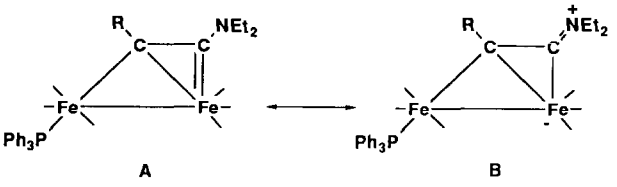

Scheme 4.

As expected from the fact that triphenylphosphine replaces a CO on the "$Fe(CO)_4$" group, the carbene structure is preserved. The ^1H and ^{13}C NMR spectra of **2d** are very similar to those of **1d**. The ^{13}C chemical shifts of C(1) in both complexes are identical (**1d**: 227.3 ppm; **2d**: 227.5 ppm). The signal at 215 ppm is assigned to equivalent carbonyl groups. This single carbonyl resonance indicates a dynamic averaging of CO ligands at 25°C. At −50°C, only four resonances are observed, in an intensity ratio 1:2:2:1. A slight difference is observed for the bridging carbene, C(2), which is shifted upfield by 4.1 ppm. This difference may be related to the *trans* position of PPh_3 with respect to C(2), as discussed above. As in **1**, complex **2** may be represented by the two resonance structures A and B (Scheme 4).

3. Experimental section

3.1. General procedure

All reactions were carried out under an inert atmosphere of dry dinitrogen or argon using standard Schlenk or vacuum line techniques. Hexane and dichloromethane were purified by standard procedures and stored over molecular sieves. PPh_3 was obtained from Aldrich Chemical Co. Complexes **1** $[Fe_2(CO)_7\{\mu\text{-}C(R)C(NEt_2)\}]$ (R = Me, C_3H_5, $SiMe_3$, or Ph) were prepared by previously reported procedures [1,2d,4]. Preparative column chromatographies were performed on 70-230 mesh Merck silica gel. IR spectra (KBr pellet) were recorded on a Nicolet Magna 550 spectrophotometer. The NMR spectra (^1H, ^{13}C, ^{31}P) were recorded on a Bruker AC 300 spectrometer. A Nermag $R_{10\text{-}10}$ spectrometer was used for molecular ion mass

determinations. Microanalyses were obtained from the Analytical Service of the Université Pierre et Marie Curie.

3.2. Preparation of complexes (2)

The synthetic procedures were similar for the four complexes. Triphenylphosphine (1 equiv) was added to a solution of complex **1** in hexane. The reaction mixture was stirred for 2 h at room temperature. The hexane is removed *in vacuo* affording a crude orange product. Further purification can be carried out by recrystallization from hexane at −10°C or by column chromatography on silica gel.

3.2.1. $[Fe_2(CO)_6PPh_3\{C(CH_3)C(NEt_2)\}]$ (2a)

2a was purified by column chromatography (dichloromethane/hexane, 10/90, as eluent). Orange crystals (yield 70%) mp = 154–155°C. IR and NMR spectra are listed in Table 2. Anal calcd. for $C_{31}H_{28}Fe_2NO_6P$: C, 56.99; H, 4.29; N, 2.14. Found: C, 57.12, H, 4.46, N, 2.17%.

3.2.2. $[Fe_2(CO)_6PPh_3\{C(C_3H_5)C(NEt_2)\}]$ (2b)

2b was obtained as red crystals (yield 80%) by recrystallization from hexane at −20°C mp = 148–150°C. IR and NMR spectra are listed in Table 2. Anal. calcd. for $C_{33}H_{30}Fe_2NO_6P$: C, 58.35; H, 4.45; N, 2.06. Found: C, 58.36, H, 4.48, N, 1.99%

3.2.3. $Fe_2(CO)_6PPh_3\{C(SiMe_3)C(NEt_2)\}]$ (2c)

2c was obtained as orange-red crystals (yield 80%) by recrystallization from hexane at −20°C, mp = 160°C. IR and NMR spectra are listed in Table 2. Anal. calcd. for $C_{33}H_{34}Fe_2NO_6PSi$: C, 55.71; H, 4.81; N, 2.07. Found: C, 55.75, H, 4.93, N, 1.97%.

3.2.4. $[Fe_2(CO)_6PPh_3\{C(Ph)C(NEt_2)\}]$ (2d)

2d was purified by column chromatography (dichloromethane/hexane, 90/10, as eluent). Orange crystals (yield 85%) mp = 164°C. IR and NMR spectra are listed in Table 2. Anal. calcd. for $C_{36}H_{30}Fe_2NO_6P$: C,

TABLE 5. Crystallographic data

Crystal Parameters		
Compound	**1d**, $C_{19}H_{15}NO_7Fe_2$	**2d**, $C_{36}H_{30}NO_6PFe_2$
fw	481.02	715.3
Crystal system	triclinic	monoclinic
Space group	$P1/$	$P2_1/n$
a (Å)	9.208(4)	10.210(6)
b (Å)	10.263(2)	16.471(7)
c (Å)	10.962(1)	20.414(8)
α (deg)	93.64(1)	
β (deg)	92.18(2)	99.78(5)
γ (deg)	92.12(3)	
V(A^3)	1032(6)	3383(31)
Z	2	4
ρ (calcd) (g cm^{-3})	1.55	1.40
μ (Mo Kα) (cm^{-1})	14.42	9.47
Data Collection		
Diffractometer	Philips PW1100	Nonius CAD4F
Monochromator	graphite	graphite
Radiation	Mo Kα(λ = 0.71069)	Mo Kα(λ = 0.71069)
Scan type	$\omega/2\theta$	$\omega/2\theta$
Scan range θ (deg)	0.8 + 0.345 tan θ	0.80 + 0.345 tan θ
2θ range (deg)	$2 < 2\theta < 50$	$3 < 2\theta < 50$
Reflctn collected	3614	7060
Reflctn merged (Rm)	3404(0.013)	6583(0.052)
Reflctn used ($I > 3\sigma(I)$)	2857	2281
Refinement		
R	0.028	0.044
R_w	0.028	0.052
Abs. corr.	DIFABS	DIFABS
Min./max. abs.	0.982–1.037	0.960–1.048
Weighting scheme	unity	Chebyshev
Coeff. Ar		5.83; −2.55; 4.40
I.s. parameters	263	416

60.59; H, 4.21; N, 1.96. Found: C, 60.70, H, 4.35, N, 1.92%.

3.3. Crystallographic analyses

For **1d** and **2d** a selected crystal was mounted on an automatic diffractometer. Unit cell dimensions with estimated standard deviations were obtained from least-squares refinements of the setting angles of 25 well centred reflections. Two standard reflections were monitored periodically; they showed no change during data collection carried out at room temperature (21°C). Crystallographic data and other pertinent information are summarized in Table 5. Corrections were made for Lorentz and polarization effects. Absorption corrections (DIFABS [11]) were applied.

Computations were performed by using CRYSTALS [12] adapted to a MicroVax II. Atomic form factors for neutral Fe, P, N, O, C and H atoms were taken from ref. 13. Anomalous dispersion was applied. The two structures were solved by direct methods using the SHELX86 program [14]. Hydrogen atoms were located on difference Fourier syntheses, but the H coordinates were introduced in the refinement as fixed contributions in calculated positions. Their atomic coordinates were recalculated after each cycle. They were assigned isotropic thermal parameters 20% higher than those of the carbon to which they were attached. Anisotropic temperature factors were introduced for all non-hydrogen atoms. Least-squares refinements with an approximation to the normal matrix (three blocks) were carried out by minimizing the function $\Sigma w(|F_o| - |F_c|)^2$, where F_o and F_c are the observed and calculated

TABLE 6. Fractional atomic coordinates with e.s.d.'s in parentheses for **1d**, and equivalent isotropic thermal parameter U_{eq} (A^2) $U_{eq} = [U(11)*U(22)*U(33)]^{1/3}$

	x	y	z	U_{eq}
Fe(1)	0.44738(4)	0.73777(4)	0.79789(4)	0.0427
Fe(2)	0.17822(4)	0.65827(4)	0.73487(4)	0.0413
C(1)	0.2245(3)	0.7870(3)	0.6276(2)	0.0422
C(2)	0.2722(3)	0.8393(3)	0.7429(2)	0.0398
C(211)	0.2298(3)	0.9695(3)	0.7954(2)	0.0408
C(212)	0.0888(3)	0.9887(3)	0.8311(3)	0.0528
C(213)	0.0469(4)	1.1105(3)	0.8746(3)	0.0634
C(214)	0.1439(4)	1.2150(3)	0.8843(3)	0.0652
C(215)	0.2848(4)	1.1977(3)	0.8502(4)	0.0666
C(216)	0.3277(3)	1.0761(3)	0.8068(3)	0.0569
N(1)	0.2149(3)	0.8284(2)	0.5174(2)	0.0510
C(111)	0.1380(4)	0.7494(4)	0.4162(3)	0.0665
C(112)	0.2372(6)	0.6825(5)	0.3292(4)	0.0954
C(121)	0.2901(4)	0.9539(3)	0.4887(3)	0.0642
C(122)	0.1888(5)	1.0646(4)	0.4831(4)	0.0844
C(11)	0.4829(3)	0.6854(3)	0.6408(3)	0.0597
O(11)	0.5139(3)	0.6537(3)	0.5449(2)	0.0828
C(12)	0.6031(3)	0.8482(3)	0.8093(3)	0.0553
O(12)	0.7034(3)	0.9166(3)	0.8160(3)	0.0772
C(13)	0.3918(3)	0.7893(3)	0.9502(3)	0.0501
O(13)	0.3570(3)	0.8242(2)	1.0441(2)	0.0671
C(14)	0.5158(4)	0.5859(3)	0.8460(3)	0.0639
O(14)	0.5583(3)	0.4889(3)	0.8726(3)	0.0916
C(21)	−0.0121(4)	0.6617(3)	0.7084(3)	0.0577
O(21)	−0.1353(3)	0.6635(3)	0.6920(3)	0.0824
C(22)	0.1574(3)	0.6094(3)	0.8887(3)	0.0531
O(22)	0.1400(3)	0.5792(3)	0.9857(2)	0.0777
C(23)	0.2049(4)	0.5035(3)	0.6556(3)	0.0572
O(23)	0.2207(3)	0.4064(3)	0.6016(3)	0.0872

TABLE 7. Fractional atomic coordinates with e.s.d.'s in parentheses for **2d**, and equivalent isotropic thermal paremeter U_{eq} (A^2) $U_{eq} = [U(11)*U(22)*U(33)]^{1/3}$

	x	y	z	U_{eq}
Fe(1)	0.14695(9)	0.19657(6)	−0.00490(5)	0.0347
Fe(2)	0.0738(1)	0.33645(6)	0.04141(5)	0.0406
P(3)	0.2101(2)	0.1945(1)	−0.10499(9)	0.0382
C(1)	−0.0275(7)	0.2533(4)	0.0706(3)	0.0370
C(2)	0.1028(6)	0.2257(4)	0.0848(3)	0.0324
N(1)	−0.1460(6)	0.2291(4)	0.0780(3)	0.0521
C(111)	−0.2651(8)	0.2777(7)	0.0515(6)	0.0735
C(112)	−0.288(1)	0.3436(8)	0.0970(7)	0.1067
C(121)	−0.1661(9)	0.1446(6)	0.1035(5)	0.0746
C(122)	−0.241(1)	0.141(1)	0.1571(7)	0.1246
C(211)	0.1653(6)	0.2011(4)	0.1523(3)	0.0388
C(212)	0.1211(8)	0.2333(6)	0.2081(4)	0.0560
C(213)	0.1770(9)	0.2104(6)	0.2724(4)	0.0600
C(214)	0.2795(8)	0.1544(6)	0.2823(4)	0.0592
C(215)	0.3230(9)	0.1221(6)	0.2286(4)	0.0646
C(216)	0.2691(7)	0.1445(5)	0.1636(4)	0.0483
C(311)	0.3583(7)	0.1347(4)	−0.1135(4)	0.0398
C(312)	0.4388(8)	0.1014(5)	−0.0605(4)	0.0549
C(313)	0.5586(8)	0.0640(6)	−0.0685(4)	0.0672
C(314)	0.5940(8)	0.0592(5)	−0.1296(4)	0.0614
C(315)	0.511(1)	0.0878(6)	−0.1838(5)	0.0663
C(316)	0.3930(9)	0.1258(6)	−0.1765(4)	0.0599
C(321)	0.0869(7)	0.1516(4)	−0.1722(3)	0.0366
C(322)	0.0460(8)	0.1893(5)	−0.2320(4)	0.0569
C(323)	−0.047(1)	0.1513(6)	−0.2809(4)	0.0669
C(324)	−0.0942(8)	0.0756(6)	−0.2694(4)	0.0637
C(325)	−0.0523(9)	0.0373(5)	−0.2108(5)	0.0675
C(326)	0.0401(9)	0.0748(5)	−0.1615(4)	0.0583
C(331)	0.2532(7)	0.2941(4)	−0.1336(4)	0.0462
C(332)	0.1576(8)	0.3524(5)	−0.1502(4)	0.0530
C(333)	0.188(1)	0.4297(5)	−0.1683(5)	0.0715
C(334)	0.321(1)	0.4511(6)	−0.1678(6)	0.0849
C(335)	0.419(1)	0.3937(6)	−0.1465(7)	0.0853
C(336)	0.3852(9)	0.3149(5)	−0.1308(6)	0.0695
C(11)	−0.0207(7)	0.2086(5)	−0.0485(4)	0.0473
O(11)	−0.1263(5)	0.2097(4)	−0.0795(3)	0.0618
C(12)	0.1456(6)	0.0919(5)	0.0095(3)	0.0385
O(12)	0.1437(5)	0.0241(3)	0.0230(3)	0.0622
C(13)	0.3136(7)	0.2247(5)	0.0306(4)	0.0490
O(13)	0.4181(5)	0.2430(4)	0.0551(3)	0.0686
C(21)	0.0676(7)	0.4006(5)	0.1084(4)	0.0480
O(21)	0.0644(6)	0.4416(4)	0.1542(3)	0.0718
C(22)	0.224(1)	0.3840(6)	0.0249(5)	0.0697
O(22)	0.3184(8)	0.4165(4)	0.0178(5)	0.0976
C(23)	−0.038(1)	0.3885(5)	−0.0204(4)	0.0569
O(23)	−0.1211(8)	0.4206(4)	−0.0568(3)	0.0791

structure factors. The weighting scheme used in the last refinement cycles was unit weights for **1d** and $w = w'[1 - (\Delta F/6\sigma(F_o))^2]^2$ where $w' = 1/\Sigma_1^r A_r T_r(x)$ with three coefficients A_r for the Chebyshev polynomial $A_r T_r(x)$ where x was F_c/F_c(max) [15] for **2d**. Models reached convergence with $R = \Sigma(\| F_o | - | F_c \|)/\Sigma | F_o |$ and $R_w = [\Sigma_w(| F_o | - | F_c |)^2/\Sigma_w(F_o)^2]^{1/2}$ having values listed in Table 5. Criteria for a satisfactory complete analysis were the ratios of rms shift to standard deviation being less than 0.1 and no significant features in final difference maps. The final fractional atomic coordinates are listed in Table 6 and 7.

Supplementary material available

Anisotropic thermal parameters, idealized coordinates for H atoms, and tables of bond lengths and bond angles, are available from the Cambridge Crystallographic Data Centre, or plus structure factor tables, from the authors.

References

1 E. Cabrera, J.C. Daran, Y. Jeannin and O. Kristiansson, *J. Organomet. Chem., 310* (1986) 367.
2 (a) M. Gouygou, J.C. Daran, B. Heim and Y. Jeannin, *J. Organomet. Chem., 460* (1993) 219; (b) R.D. Adams, J.C. Daran and Y. Jeannin, *C.R. Acad. Sci. Paris, 312* (1991) 1117; (d) V. Crocq, J.C. Daran, Y. Jeannin, B. Eber and G. Huttner, *Organometallics 10*, (1991) 448; (e) V. Crocq, J.C. Daran and Y. Jeannin, *J. Organomet. Chem., 313* (1989) 8; (f) E. Cabrera, J.C. Daran and Y. Jeannin, *Organometallics, 7* (1988) 2010.
3 A.A. Low and J.W. Lauher, *Inorg. Chem., 26* (1987) 3863.
4 J.C. Daran, B. Heim, Y. Jeannin, B. Eber, G. Huttner and W. Imhof, *J. Organomet. Chem., 441* (1992) 81.
5 B. Heim, *Thesis*, University of Paris VI, 1992.
6 M. Audouin, E. Chelain, A. Parlier, H. Rudler, J.C. Daran and J. Vaissermann, *J. Am. Chem. Soc., 115* (1993) 10568.
7 R.D. Adams, G. Chen and J. Yin, *Organometallics, 10* (1991) 1278.
8 A.E. Ogilvy, M. Draganjac, T.B. Rauchfuss and S.R. Wilson, *Organometallics, 7* (1988) 1171.
9 R. Yanez, J. Ros, F. Dahan and R. Mathieu, *Organometallics, 9* (1990) 2484.
10 W.F. Smith, J. Yule, N.J. Taylor, H.N. Paik and A.J. Carty, *Inorg. Chem., 16* (1977) 1593.
11 N. Walker and D. Stuart, *Acta Crystallogr., 39* (1983) 158.
12 D.J. Watkin, J.R. Carruthers and P.W. Betteridge, CRYSTALS *User Guide*, Chemical Crystallography Laboratory, University of Oxford, 1985.
13 *International Tables for X-ray Crystallography*, Vol. IV, Kynoch, Birmingham, 1974.
14 G.M. Sheldrick, SHELXS86, *Program for Crystal Structure Solution*, University of Göttingen, Germany, 1986.
15 E. Prince, *Mathematical Techniques in Crystallography*, 1982, Springer, Berlin.